A new MITC finite element method for the Reissner–Mindlin plate problem based on a biorthogonal system

B. P. Lamichhane[1] M. H. Meylan[2]

(Received 30 January 2017; revised 16 June 2017)

Abstract

We present a new MITC (Mixed Interpolated Tensorial Components) finite element method for Reissner–Mindlin plate equations. The new finite element method uses a biorthogonal system to construct the reduction operator for the MITC element. Numerical results are shown to demonstrate the performance of the approach.

Subject class: 65N30, 74K20

Keywords: Reissner–Mindlin plate, finite element, Lagrange multiplier, biorthogonal system, a priori error estimates

DOI:10.21914/anziamj.v58i0.11754, © Austral. Mathematical Soc. 2017. Published July 16, 2017, as part of the Proceedings of the 18th Biennial Computational Techniques and Applications Conference. ISSN 1445-8810. (Print two pages per sheet of paper.)

Contents

1 Introduction

Reissner–Mindlin plate or shell equations are often used to compute the deformation of a thin plate or shell under some external forces. Some useful industrial applications for Reissner–Mindlin plate equations include crash simulation of cars, optimisation of wind-turbines and ice shelf modelling. Since these equations are not analytically solvable in most applications, finite element methods are employed to compute the approximate solution of these equations. The Reissner–Mindlin plate or shell equations model the thin plate or shell with a parameter for the thickness of the plate or shell, consequently it is challenging to develop a numerical method which converges uniformly when the plate or shell thickness parameter approaches zero.

It is well known that standard finite element discretisations of the Reissner–Mindlin plate equations do not converge uniformly with respect to the plate thickness [5, 6], which is often known as *shear* or *membrane* locking. Therefore, most of the finite element methods which converge uniformly for the Reissner–Mindlin plate equations are based on mixed finite element methods [1, 3, 4, 6, 12, 16, 17].

The MITC (Mixed Interpolated Tensorial Components) technique, which is based on using a reduction operator, is one of the most popular finite element techniques [11, 18]. Although the MITC technique is often analysed as a mixed finite element approach for the Reissner–Mindlin plate equations, the reduction operator of the MITC technique enables a positive definite finite element formulation. The reduction operator is a projection onto a finite element space, and its stability and approximation property is crucial in the analysis.

We propose an efficient finite element method to obtain a uniform approximation of the Reissner–Mindlin plate equations utilising the reduction operator as proposed in the MITC technique. Our reduction operator is constructed by using a biorthogonal system and is thus an oblique projection operator onto the standard finite element space. A related approach using a biorthogonal system has been previously proposed by Lamichhane [15]. This approach of Lamichhane [15] does not use the MITC formulation and also involves a complicated boundary modification procedure for the clamped boundary condition. Our new approach does not involve a boundary modification and has a simpler formulation than the earlier approach.

Section 2 briefly summarises the Reissner–Mindlin plate equations in a modified form as given by Arnold and Brezzi [1], and we propose a new constrained minimisation formulation upon which the MITC technique is based. Section 3 describes our MITC finite element method based on a biorthogonal system. Finally, we present some numerical results that show the performance of the numerical scheme, in particular, that the numerical scheme converges uniformly with plate thickness in Section 4.

2 A mixed formulation for Reissner–Mindlin plates

Let $\Omega \subset \mathbb{R}^2$ be a bounded region with polygonal boundary. We use standard notations for Sobolev spaces [6, 8], where $L^2(\Omega)$ denotes the set of all square integrable functions in the sense of Lebesgue. The norm on the Lebesgue space $L^2(\Omega)$ is defined as

$$\|u\|_{L^2(\Omega)} = \sqrt{\int_\Omega u^2 \, dx}\,.$$

The standard Sobolev space $H^1(\Omega)$ is the space of all square integrable functions whose first-order partial derivatives are also square integrable:

$$H^1(\Omega) = \left\{ u \in L^2(\Omega) : \frac{\partial u}{\partial x_i} \in L^2(\Omega),\ i = 1, 2 \right\}.$$

The norm on the Sobolev space $H^1(\Omega)$ is defined as

$$\|u\|_{H^1(\Omega)} = \sqrt{\int_\Omega u^2 \, dx + \int_\Omega \|\nabla u\|^2 \, dx}\,,$$

where $\|\cdot\|$ is the standard Euclidean norm on $\mathbb{R}^2$. More details about these norms are given by Braess [6] and Brenner and Scott [8]. We now introduce the following vector Sobolev spaces for the variational formulation of the Reissner–Mindlin plate problem:

$$\mathbb{H}^1(\Omega) = [H^1(\Omega)]^2, \quad \mathbb{H}^1_0(\Omega) = [H^1_0(\Omega)]^2, \quad \text{and} \quad \mathbb{L}^2(\Omega) = [L^2(\Omega)]^2.$$

The norm on the spaces $\mathbb{H}^1(\Omega)$ and $\mathbb{L}^2(\Omega)$ have the same notation as the spaces $H^1(\Omega)$ and $L^2(\Omega)$, respectively.

We consider the following formulation of the Reissner–Mindlin plate with clamped boundary condition [1, 3, 12]. The Reissner–Mindlin plate problem

is to find the transverse displacement of the mid-plane section Ω of the plate denoted by $\mathfrak{u}$ and the rotation $\boldsymbol{\phi}$ of the transverse normal vector. The transverse displacement of the mid-plane section Ω of the plate is the displacement along the z-direction of the plate, as shown in the bottom panel of Figure 1. Using the modification proposed by Arnold and Brezzi [1] the Reissner–Mindlin problem is to find $(\boldsymbol{\phi}, \mathfrak{u}) \in \mathbb{H}^1_0(\Omega) \times \mathsf{H}^1_0(\Omega)$ such that

$$\mathfrak{a}(\boldsymbol{\phi}, \mathfrak{u}; \boldsymbol{\psi}, \nu) = \ell(\nu), \quad (\boldsymbol{\psi}, \nu) \in \mathbb{H}^1_0(\Omega) \times \mathsf{H}^1_0(\Omega)\,, \tag{1}$$

where

$$\begin{aligned}\mathfrak{a}(\boldsymbol{\phi}, \mathfrak{u}; \boldsymbol{\psi}, \nu) = &\int_\Omega \mathcal{C}\boldsymbol{\epsilon}(\boldsymbol{\phi}) : \boldsymbol{\epsilon}(\boldsymbol{\psi})\, d\mathbf{x} + \lambda \int_\Omega (\boldsymbol{\phi} - \nabla \mathfrak{u}) \cdot (\boldsymbol{\psi} - \nabla \nu)\, d\mathbf{x} \\ &+ \frac{\lambda(1-\mathsf{t}^2)}{\mathsf{t}^2} \int_\Omega (\boldsymbol{\phi} - \nabla \mathfrak{u}) \cdot (\boldsymbol{\psi} - \nabla \nu)\, d\mathbf{x}\,,\end{aligned} \tag{2}$$

and

$$\ell(\nu) = \int_\Omega \mathsf{g}\, \nu\, d\mathbf{x}\,.$$

Here $\mathsf{t} < 1$ is the plate thickness, λ is a material constant depending on Young's modulus E and Poisson's ratio ν as

$$\lambda = \frac{5\mathsf{E}}{12(1+\nu)}\,,$$

and g is the body force. Moreover, $\boldsymbol{\epsilon}(\boldsymbol{\phi})$ is the symmetric part of the gradient,

$$\boldsymbol{\epsilon}(\boldsymbol{\phi}) = \frac{\nabla \boldsymbol{\phi} + [\nabla \phi]^\mathsf{T}}{2}\,,$$

and $\mathcal{C}$ is the fourth-order elasticity tensor

$$\mathcal{C}\mathbf{d} = \frac{\mathsf{E}}{12(1-\nu^2)} \left[(\nu \operatorname{tr} \mathbf{d})\mathbf{1} + (1-\nu)\,\mathbf{d}\right], \quad \mathbf{d} \in [\mathsf{L}^2(\Omega)]^{2\times 2}\,,$$

where $\mathbf{1}$ is the second-order identity tensor and $\operatorname{tr} \mathbf{d}$ is the trace of the symmetric tensor $\mathbf{d}$. Since the bilinear form $\mathfrak{a}(\cdot,\cdot)$ is continuous and coercive [1, 6],

and the right-hand side $\ell(\cdot)$ is continuous if $g \in H^{-1}(\Omega)$, problem (1) has a unique solution from the Lax–Milgram lemma.

We now recast the Reissner–Mindlin problem as a minimisation problem of finding $(\boldsymbol{\phi}, u) \in \mathbb{H}^1_0(\Omega) \times H^1_0(\Omega)$ such that

$$(\boldsymbol{\phi}, u) = \underset{(\boldsymbol{\psi}, v) \in \mathbb{H}^1_0(\Omega) \times H^1_0(\Omega)}{\arg\min} \tfrac{1}{2} a(\boldsymbol{\psi}, v; \boldsymbol{\psi}, v) - \ell(v)\,.$$

Constrained minimisation formulation

Introducing a new unknown

$$\boldsymbol{\zeta} = \frac{\sqrt{\lambda(1-t^2)}}{t}(\boldsymbol{\phi} - \nabla u) \in \mathbb{L}^2(\Omega),$$

then as shown by Braess [6] we minimize the functional

$$J(\boldsymbol{\phi}, u, \boldsymbol{\zeta}) = \frac{1}{2}\left[A(\boldsymbol{\phi}, u) + \int_\Omega \boldsymbol{\zeta} \cdot \boldsymbol{\zeta}\, dx\right] - \ell(u)\,, \tag{3}$$

over $\mathbb{H}^1_0(\Omega) \times H^1_0(\Omega)$ with

$$A(\boldsymbol{\phi}, u) = \int_\Omega \mathcal{C}\boldsymbol{\epsilon}(\boldsymbol{\phi}) : \boldsymbol{\epsilon}(\boldsymbol{\phi})\, dx + \lambda \int_\Omega (\boldsymbol{\phi} - \nabla u) \cdot (\boldsymbol{\phi} - \nabla u)\, dx$$

subject to the constraint

$$\int_\Omega \boldsymbol{\zeta} \cdot \boldsymbol{\eta}\, dx = \frac{\sqrt{\lambda(1-t^2)}}{t} \int_\Omega (\boldsymbol{\phi} - \nabla u) \cdot \boldsymbol{\eta}\, dx, \quad \boldsymbol{\eta} \in \mathbb{L}^2(\Omega)\,. \tag{4}$$

The main benefit of using this modified formulation proposed by Arnold and Brezzi [1] is that the bilinear form $A(\cdot,\cdot)$ satisfies the coercivity condition

$$A(\boldsymbol{\phi}, u) \geqslant C\left(\|\boldsymbol{\phi}\|^2_{H^1(\Omega)} + \|u\|^2_{H^1(\Omega)}\right)$$

on the whole space $\mathbb{H}^1_0(\Omega) \times H^1_0(\Omega)$, which is not true for the original formulation [6].

3 Finite element discretisation

We consider a quasi-uniform triangulation $\mathcal{T}_h$ of the polygonal domain Ω with mesh-size h, where $\mathcal{T}_h$ consists of triangles or parallelograms. Given a triangulation $\mathcal{T}_h$, we introduce the standard linear finite element space

$$K_h := \{v \in H^1(\Omega) : v_{|_T} \in \mathcal{P}_1(T)\,, T \in \mathcal{T}_h\}\,,$$

and let $S_h := H_0^1(\Omega) \cap K_h$. We use the finite element space S_h for the transverse displacement and $\mathbf{V}_h := [S_h]^2$ for the rotation.

In order to construct the reduction operator for the MITC element we construct another piecewise polynomial space M_h, where the basis functions $\{\mu_1, \mu_2, \ldots, \mu_n\}$ of M_h and the basis functions $\{\varphi_1, \varphi_2, \ldots, \varphi_n\}$ of K_h form a biorthogonal system so that

$$\int_\Omega \mu_i\ \varphi_j\, dx = c_j \delta_{ij}\,, \quad 1 \leqslant i, j \leqslant n\,, \tag{5}$$

where $n := \dim M_h = \dim K_h$, δ_{ij} is the Kronecker symbol, and c_j is a nonzero scaling factor. We construct local basis functions [13, 14] for M_h on the reference triangle $\hat{T}$ so that for the reference triangle $\hat{T} := \{(x, y) : 0 \leqslant x, 0 \leqslant y, x + y \leqslant 1\}$ we have three vertex basis functions

$$\hat{\mu}_1 := 3 - 4x - 4y\,, \quad \hat{\mu}_2 := 4x - 1\,, \quad \hat{\mu}_3 := 4y - 1\,.$$

Using the main idea of MITC elements [18], we introduce a reduction operator $R_h : L^2(\Omega) \to S_h$ defined as

$$\int_\Omega R_h v\, \mu_h\, dx = \int_\Omega v\, \mu_h\, dx\,, \quad \mu_h \in M_h\,. \tag{6}$$

Due to the biorthogonality relation the application of the reduction operator R_h to a function $v \in L^2(\Omega)$ has a closed form representation as

$$R_h v = \sum_{i=1}^{n} \frac{\int_\Omega \mu_i\, v\, dx}{c_i} \varphi_i\,.$$

This expression is also useful for the numerical implementation.

The reduction operator R_h is a quasi-projection operator having the properties listed in the following lemma. In the following lemma, we use a generic constant C, which takes different values at different places but is always independent of the mesh-size h.

Lemma 1. *Let* $R_h : L^2(\Omega) \to S_h$ *be defined by* (6). *Then* R_h *has the following properties.*

1. **Stability in L^2-norm:** *Since* $\dim M_h = \dim S_h$, *if* $v \in L^2(\Omega)$ *then*

$$\|R_h v\|_{L^2(\Omega)} \leqslant C\|v\|_{L^2(\Omega)}. \tag{7}$$

2. **Stability in H^1-norm:** *Similarly, if* $v \in H^1(\Omega)$ *then*

$$\|R_h v\|_{H^1(\Omega)} \leqslant C\|v\|_{H^1(\Omega)}. \tag{8}$$

3. **Approximation property:** *If* $v \in H^{s+1}(\Omega)$ *and* $0 < s \leqslant 1$ *then*

$$\begin{cases} \|v - R_h v\|_{L^2(\Omega)} & \leqslant & Ch^{1+s}|v|_{H^{s+1}(\Omega)}, \\ \|v - R_h v\|_{H^1(\Omega)} & \leqslant & Ch^{s}|v|_{H^{s+1}(\Omega)}. \end{cases} \tag{9}$$

Kim et al. [13] and Lamichhane [14] proved this lemma, where R_h is introduced as the mortar projection operator. The definition of the Sobolev space $H^s(\Omega)$ for $s > 0$ and its associated norm $\|\cdot\|_{H^s(\Omega)}$ are given by Brenner and Scott [8].

A new finite element method

Using the MITC technique with the reduction operator R_h our finite element method for the Reissner–Mindlin problem is to find $(\boldsymbol{\phi}_h, u_h) \in \mathbf{V}_h \times S_h$ such that

$$a_h(\boldsymbol{\phi}_h, u_h; \boldsymbol{\psi}_h, v_h) = \ell(v_h), \quad (\boldsymbol{\psi}_h, v_h) \in \mathbf{V}_h \times S_h, \tag{10}$$

where

$$a_h(\boldsymbol{\phi}_h, u_h; \boldsymbol{\psi}_h, v_h) = \int_\Omega \mathcal{C}\boldsymbol{\epsilon}(\boldsymbol{\phi}_h) : \boldsymbol{\epsilon}(\boldsymbol{\psi}_h)\, d\mathbf{x} + \lambda \int_\Omega (\boldsymbol{\phi}_h - \nabla u_h) \cdot (\boldsymbol{\psi}_h - \nabla v_h)\, d\mathbf{x} + \frac{\lambda(1-t^2)}{t^2} \int_\Omega R_h(\boldsymbol{\phi}_h - \nabla u_h) \cdot R_h(\boldsymbol{\psi}_h - \nabla v_h)\, d\mathbf{x}\,. \tag{11}$$

Remark 2. Working with $\mathbf{V}_h \subset \mathbb{H}^1(\Omega)$, $S_h \subset H_0^1(\Omega)$ and $[M_h]^2 \subset \mathbb{L}^2(\Omega)$ in (4), for $\zeta_h \in K_h$ then

$$\int_\Omega \zeta_h \cdot \boldsymbol{\eta}_h\, d\mathbf{x} = \frac{\sqrt{\lambda(1-t^2)}}{t} \int_\Omega (\boldsymbol{\phi}_h - \nabla u_h) \cdot \boldsymbol{\eta}_h\, d\mathbf{x}, \quad \boldsymbol{\eta}_h \in [M_h]^2\,, \tag{12}$$

which yields

$$\zeta_h = \frac{\sqrt{\lambda(1-t^2)}}{t} R_h(\boldsymbol{\phi}_h - \nabla u_h)\,.$$

Since R_h is a projection operator onto $\mathbf{V}_h$, we write

$$R_h(\boldsymbol{\phi}_h - \nabla u_h) = \boldsymbol{\phi}_h - R_h \nabla u_h\,.$$

Since u_h is piecewise linear, ∇u_h becomes a piecewise constant vector function with respect to the underlying mesh $\mathcal{T}_h$. Then $R_h \nabla u_h$ is the projection of this piecewise constant vector function back to the piecewise linear vector function.

Enriching the finite element space with bubble functions

The above finite element method is similar to the P_1-P_1 mixed finite element approach for the Stokes equations. To obtain stability the P_1-P_1 mixed finite element approach is often modified by enriching the finite element space

for the velocity with the space of bubble functions [2]. In the case of the Reissner–Mindlin plate equations the space of transverse displacement is enriched with the bubble functions [1, 15]. Following similar lines we compare the above finite element approach with the method where the finite element space for the transverse displacement field is enriched with the space of bubble functions

$$B_h := \left\{ b_T \in \mathcal{P}_3(T) : b_{T|_{\partial T}} = 0 \,, \int_T b_T \, d\mathbf{x} > 0, \, T \in \mathcal{T}_h \right\} ,$$

and $\mathcal{P}_3(T)$ is the space of cubic polynomials in T. The bubble function on an element T is defined as

$$b_T(x) = c_b \prod_{i=1}^{3} \lambda_{T^i}(x),$$

where $\lambda_{T^i}(x)$ are the barycentric coordinates of the element T associated with vertices x_{T^i} of T, $i = 1, 2, 3$, and the constant c_b is chosen in such a way that the value of b_T at the barycentre of T is one.

The new finite element space for the transverse displacement u is $S_h^B = S_h \oplus B_h$, whereas the finite element space for the rotation $\boldsymbol{\phi}$ is the same as before. Thus the problem is to find $(\boldsymbol{\phi}_h, u_h) \in \mathbf{V}_h \times S_h^B$ such that

$$a_h(\boldsymbol{\phi}_h, u_h; \boldsymbol{\psi}_h, v_h) = \ell(v_h) \,, \quad (\boldsymbol{\psi}_h, v_h) \in \mathbf{V}_h \times S_h^B \,, \tag{13}$$

where $a_h(\cdot, \cdot)$ is defined by (11).

Existence and uniqueness of solution

Since $\mathbf{V}_h \subset \mathbb{H}_0^1(\Omega)$ and S_h and S_h^B both are subsets of $H_0^1(\Omega)$, the bilinear form $a_h(\cdot, \cdot)$ and the linear form $\ell(\cdot)$ both are continuous. Moreover, independent of whether $(\boldsymbol{\phi}_h, u_h) \in \mathbf{V}_h \times S_h$ or $(\boldsymbol{\phi}_h, u_h) \in \mathbf{V}_h \times S_h^B$, the bilinear form $a_h(\cdot, \cdot)$ satisfies the coercivity condition [1]:

$$a_h(\boldsymbol{\phi}_h, u_h; \boldsymbol{\phi}_h, u_h) \geqslant C \left(\|\boldsymbol{\phi}_h\|^2_{H^1(\Omega)} + \|u_h\|^2_{H^1(\Omega)} \right) .$$

Hence both discrete problems of solving (10) or (13) have unique solutions.

For comparison we also consider the standard approach to discretise the Reissner–Mindlin plate equations, namely, find $(\boldsymbol{\phi}_h, u_h) \in \mathbf{V}_h \times S_h$ such that

$$a(\boldsymbol{\phi}_h, u_h; \boldsymbol{\psi}_h, v_h) = \ell(v_h)\,, \quad (\boldsymbol{\psi}_h, v_h) \in \mathbf{V}_h \times S_h\,, \tag{14}$$

where $a(\cdot,\cdot)$ is defined by (2). In the standard approach $a(\cdot,\cdot)$ is different from $a_h(\cdot,\cdot)$ in both MITC approaches, and it does not involve the reduction operator R_h in contrast to the MITC approach.

Although a detailed theoretical convergence study is outside the scope of this short communication, we expect the following asymptotic convergence rates for the L^2- and H^1-norms of the transverse displacement and rotation:

$$\|u - u_h\|_{L^2(\Omega)} = O(h^2), \quad \|u - u_h\|_{H^1(\Omega)} = O(h),$$
$$\|\boldsymbol{\phi} - \boldsymbol{\phi}_h\|_{L^2(\Omega)} = O(h^2), \quad \|\boldsymbol{\phi} - \boldsymbol{\phi}_h\|_{H^1(\Omega)} = O(h).$$

Here $f = O(h^k)$ means there exists a mesh-independent constant C such that $f \leqslant Ch^k$.

4 Numerical results

In this section we demonstrate the performance of our numerical methods in two selected examples. We consider three finite element methods: the standard approach given by (14), the approach with the reduction operator but without bubble functions (MITC without bubble functions) given by (10), and the approach with the reduction operator and bubble functions (MITC with bubble functions) given by (13). We used a simple direct solver based on Gaussian elimination to solve the arising linear systems of equations. However, since the arising system is symmetric, an efficient iterative solution technique could be applied [7, 10]. The computational cost for the standard approach and the MITC approach without bubble functions is the same, whereas the MITC approach with bubble functions has more degrees of freedom and therefore, is computationally more expensive than the other two approaches.

Figure 1: Initial mesh for Example 1 and 2 (top), and solution for Example 2 (bottom).

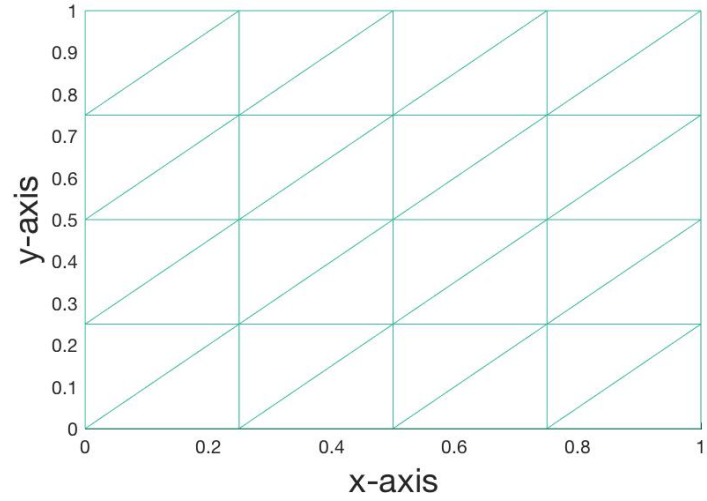

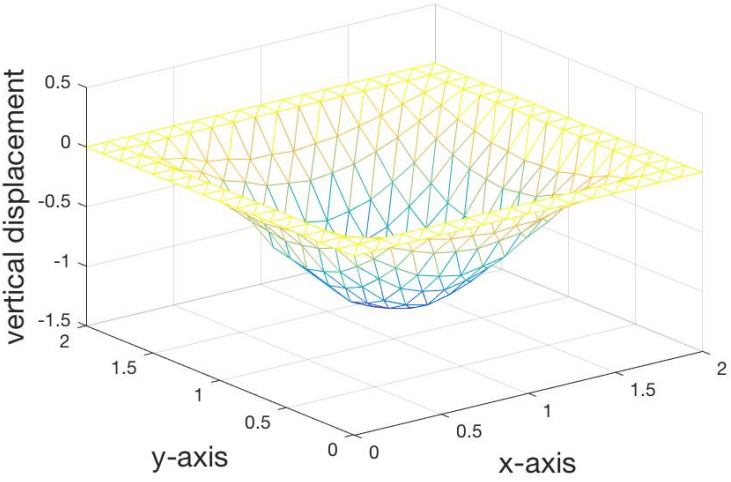

Example 1 Our first numerical example is taken from Chinosi et al. [9], where the exact solution for the transverse displacement is given by

$$u(x,y) = \frac{2\,t^2[r(x,y)+r(y,x)]}{5(\nu-1)} + \frac{x^3\,y^3\,(x-1)^3\,(y-1)^3}{3}$$

with

$$r(x,y) = x\,y^3\,(x-1)\,(y-1)^3\,\left(5\,x^2-5\,x+1\right),$$

and exact solutions for two components of rotation are

$$\begin{aligned}\phi_1(x,y) &= x^2\,y^3\,(2\,x-1)\,(x-1)^2\,(y-1)^3,\\ \phi_2(x,y) &= x^3\,y^2\,(2\,y-1)\,(x-1)^3\,(y-1)^2.\end{aligned}$$

We set $t = 0.001$ so that the plate thickness is sufficiently small. We also used the Young's modulus and Poisson's ratio as $E = 1000\,\mathrm{N/mm^2}$; $\nu = 0.3$. We have initialized the triangulations with 32 elements as shown in the top panel of Figure 1 and uniformly refined the triangulations to compute errors in various norms. Figure 2 and Figure 3 shows the L^2 and H^1 errors for the transverse displacement and rotation vector for all three finite element methods. From these figures both MITC finite element approaches yield convergence of $O(h^2)$ for the errors in the L^2-norm and of $O(h)$ for the errors in the H^1-norm for both the transverse displacement and rotation, whereas the standard approach shows very poor convergence. Also, the MITC approach without bubble functions yield lower errors than the MITC approach with bubble functions. This is expected as bubble functions do not improve the approximation of the finite element space.

Example 2 This is a well-known classical numerical example [20] for a clamped plate, which tests numerical schemes for a bending dominated situation. A thin plate of dimension $2\,\mathrm{mm} \times 2\,\mathrm{mm} \times 0.01\,\mathrm{mm}$ is considered. The plate is clamped along the complete boundary, and it is subjected to a uniformly distributed pressure of $100\,\mathrm{N/mm^2}$ on the top surface in the z-direction [19]. A linear elastic material is considered with Young's modulus

Figure 2: L^2 errors (top) and H^1 errors (bottom) versus the number of elements for the transverse displacement u of Example 1.

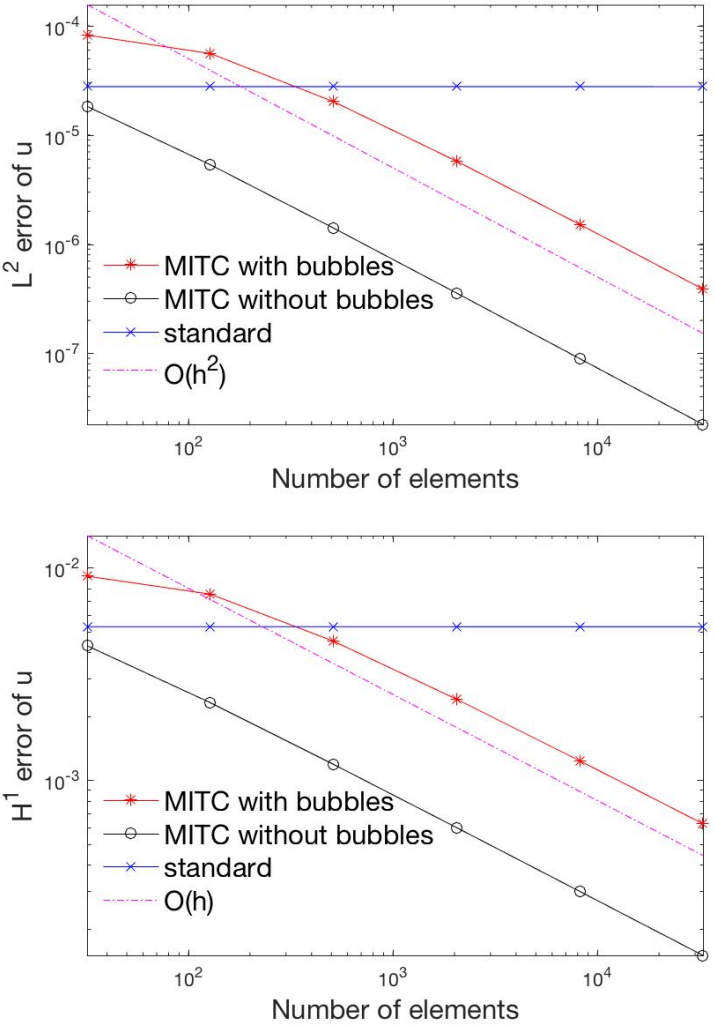

Figure 3: L^2 errors (top) and H^1 errors (bottom) versus the number of elements for the rotation ϕ of Example 1.

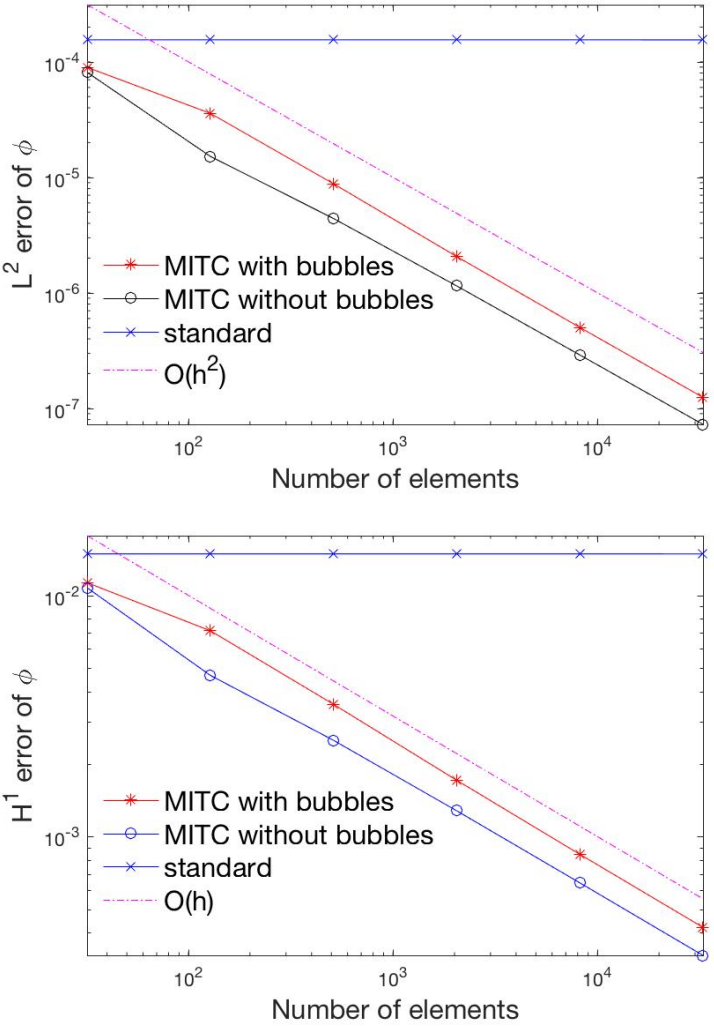

$\mathsf{E} = 1.7472 \times 10^7\,\mathrm{N/mm^2}$ and Poisson's ratio $\nu = 0.3$. Figure 1 shows the initial triangulation and the deformation of the plate. We also plotted the vertical displacement of the mid-point of the plate in the top panel of Figure 4. Both MITC approaches converge to the exact solution rapidly, whereas the standard approach has very slow convergence.

In the second part, we keep the uniform mesh with 2048 elements and compute the vertical displacement at the mid-point of the plate using different thickness measurements of the plate. The bottom panel of Figure 4 shows the numerical results with different finite element schemes. The standard scheme locks when the plate thickness gets smaller, whereas both MITC schemes show good convergence to the correct solution.

5 Conclusion

We constructed an efficient reduction operator based on a biorthogonal system for the MITC element method of Reissner–Mindlin plate equations. The numerical results demonstrate that the proposed method has uniform convergence with respect to the plate thickness. A very important future step will be to prove the uniform convergence of both finite element schemes with respect to the plate thickness.

References

[1] D. Arnold and F. Brezzi. Some new elements for the Reissner–Mindlin plate model. In J. L. Lions, C. Baiocchi and E. Magenes editors. *Boundary Value Problems for Partial Differential Equations and Applications: Dedicated to E. Magenes*. Masson, Paris, 1993, pp. 287–292. http://umn.edu/~arnold/papers/rmelts.pdf C2, C3, C4, C5, C6, C10

Figure 4: The vertical displacement at the mid-point of the plate versus the number of elements (top) and the plate thickness (bottom) for Example 2.

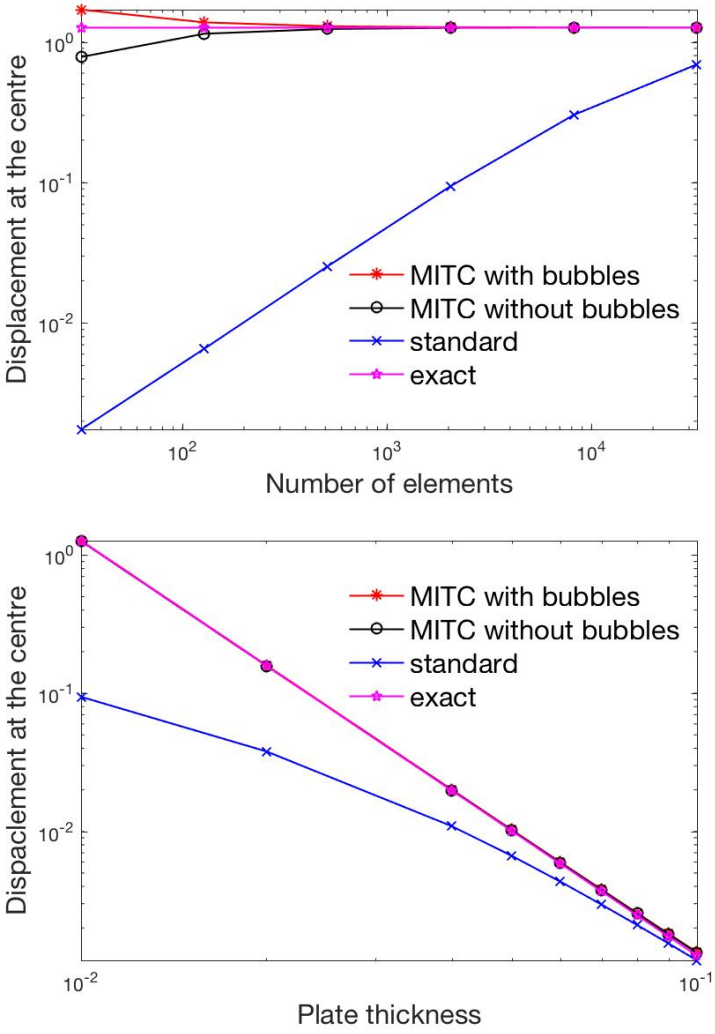

[2] D. Arnold, F. Brezzi and M. Fortin. A stable finite element for the Stokes equations. *Calcolo*, **21**:337–344, 1984. doi:10.1007/BF02576171 C10

[3] D. Arnold and R. Falk. A uniformly accurate finite element method for the Reissner–Mindlin plate. *SIAM Journal on Numerical Analysis*, **26**:1276–1290, 1989. doi:10.1137/0726074 C2, C4

[4] D. Arnold and R. Falk. Analysis of a linear-linear finite element for the Reissner–Mindlin plate model. *Mathematical Models and Methods in Applied Science*, **7**:217–238, 1997. doi:10.1142/S0218202597000141 C2

[5] D. Boffi, F. Brezzi and M. Fortin. *Mixed Finite Element Methods and Applications*. Springer–Verlag, Berlin, Heidelberg, 2013. doi:10.1007/978-3-642-36519-5 C2

[6] D. Braess. *Finite Elements. Theory, Fast Solver, and Applications in Solid Mechanics*. 2nd edition, Cambridge Univ. Press, Cambridge, 2001. doi:10.1017/CBO9780511618635 C2, C4, C5, C6

[7] S. Brenner. Multigrid methods for parameter dependent problems. *ESAIM: Mathematical Modelling and Numerical Analysis*, **30**:265–297, 1996. doi:10.1051/m2an/1996300302651 C11

[8] S. Brenner and L. Scott. *The Mathematical Theory of Finite Element Methods*. Springer–Verlag, New York, 1994. doi:10.1007/978-0-387-75934-0 C4, C8

[9] C. Chinosi, C. Lovadina and L. Marini. Nonconforming locking-free finite elements for Reissner–Mindlin plates. *Computer Methods in Applied Mechanics and Engineering*, **195**:3448–3460, 2006. doi:10.1016/j.cma.2005.06.025 C13

[10] L. B. da Veiga, C. Chinosi, C. Lovadina and L. F. Pavarino. Robust BDDC preconditioners for Reissner–Mindlin plate bending problems and MITC elements. *SIAM Journal on Numerical Analysis*, **47(6)**:4214–4238, 2010. doi:10.1137/080717729 C11

[11] E. Dvorkin and K. Bathe. A continuum mechanics based four-node shell element for general nonlinear analysis. *Engineering Computations*, **1**:77–88, 1984. doi:10.1108/eb023562 C3

[12] R. Falk and T. Tu. Locking-free finite elements for the Reissner-Mindlin plate. *Mathematics of Computation*, **69**:911–928. doi:10.1090/S0025-5718-99-01165-5 C2, C4

[13] C. Kim, R. Lazarov, J. Pasciak and P. Vassilevski. Multiplier spaces for the mortar finite element method in three dimensions. *SIAM Journal on Numerical Analysis*, **39**:519–538, 2001. doi:10.1137/S0036142900367065 C7, C8

[14] B. Lamichhane. *Higher Order Mortar Finite Elements with Dual Lagrange Multiplier Spaces and Applications*. PhD thesis, University of Stuttgart, 2006. doi:10.18419/opus-4770 C7, C8

[15] B. Lamichhane. Two simple finite element methods for Reissner–Mindlin plates with clamped boundary condition. *Applied Numerical Mathematics*, **72**:91–98, 2013. doi:10.1016/j.apnum.2013.04.005 C3, C10

[16] C. Lovadina. A new class of mixed finite element methods for Reissner-Mindlin plates. *SIAM Journal on Numerical Analysis*, **33**:2456–2467, 1996. doi:10.1137/S0036142994265061 C2

[17] C. Lovadina. A low-order nonconforming finite element for Reissner–Mindlin plates. *SIAM Journal on Numerical Analysis*, **42**:2688–2705, 2005. doi:10.1137/040603474 C2

[18] M. Lyly, J. Niiranen and R. Stenberg. A refined error analysis of MITC plate elements. *Mathematical Models and Methods in Applied Sciences*, **16**:967–977, 2006. doi:10.1142/S021820250600142X C3, C7

[19] D. Mijuca. On hexahedral finite element HC8/27 in elasticity. *Computational Mechanics*, **33**:466–480, 2004. doi:10.1007/s00466-003-0546-9 C13

[20] S. Timoshenko and J. Goodier. *Theory of Elasticity*. 3rd edition, McGraw-Hill, New York, 1970. doi:10.1017/S036839310012471X C13

Author addresses

1. **B. P. Lamichhane**, School of Mathematical & Physical Sciences , Mathematics Building–V127 , University of Newcastle , University Drive , Callaghan, NSW 2308, AUSTRALIA
mailto:Bishnu.Lamichhane@newcastle.edu.au

2. **M. H. Meylan**, School of Mathematical & Physical Sciences , Mathematics Building–VG26 , University of Newcastle , University Drive , Callaghan, NSW 2308, AUSTRALIA
mailto:Mike.Meylan@newcastle.edu.au